RESEARCH PAPER

Development And Optimization Of Baicalin Nanoparticle Loaded Oral Hydrogel For Colon-Targeted Therapy In Inflammatory Bowel Disease

Gavit Renuka Sukalal[1], Jitendra.V.Shinde[2], Ashok Bhosale[3]

[1]Department of Pharmaceutics , Shankarrao Ursal College of Pharmaceutical Sciences and Research Centre, Kharadi ,Pune
(Corresponding Author) Email : renukagavit597@gmail.com
[2]HOD of Pharmaceutics , Shankarrao Ursal College of Pharmaceutical Sciences and Research Centre, Kharadi, Pune
[3]Principal, Shankarrao Ursal College of Pharmaceutical Sciences and Research Centre,Kharadi , Pune

ABSTRACT

Objectives: To develop and optimize baicalin-loaded Eudragit S100-coated PLGA nanoparticles using Soluplus® as a novel steric stabilizer and incorporate the optimized batch into a Carbopol 974P NF oral hydrogel for pH-responsive colon-targeted delivery in inflammatory bowel disease, addressing the biopharmaceutical limitations of baicalin as a BCS Class IV drug.

Methods: Nine nanoparticle batches (NF1–NF9) were prepared by nanoprecipitation and optimized using a 3^2 full factorial design with PLGA concentration (X_1) and Soluplus® concentration (X_2) as independent variables, evaluating particle size and entrapment efficiency as responses. The optimized batch was incorporated into four Carbopol 974P NF hydrogel batches (G1–G4) and evaluated for physicochemical properties, mucoadhesion, ex vivo colonic permeation, and accelerated stability. **Results:** The quadratic models demonstrated excellent predictability (R^2 = 0.9992 and 0.9995). Batch NF8 (PLGA 1.5% w/v, Soluplus® 1.0% w/v) was selected as optimized based on desirability score of 1.000, particle size of 184.6 nm, PDI of 0.218, zeta potential of −27.6 mV, and entrapment efficiency of 86.7%, with sustained colonic release of 81.62% at 12 hours. Hydrogel batch G3 demonstrated highest steady-state flux of 107.44 µg/cm²/hr and 12-hour cumulative permeation of 68.24%. Accelerated stability studies confirmed formulation integrity over three months. **Conclusion:** The developed nanoparticle-loaded oral hydrogel offers pH-responsive colon targeting, strong mucoadhesion, and sustained drug release, presenting significant clinical potential for localized IBD therapy with reduced systemic toxicity and improved patient compliance, warranting further in vivo validation.

Keywords: Baicalin; PLGA nanoparticles; Soluplus®; Eudragit S100; colon-targeted delivery; inflammatory bowel disease; oral hydrogel; factorial design; mucoadhesion.

How to site this article : Sukalal GR, Shinde JV, Bhosale A. Development And Optimization Of Baicalin Nanoparticle Loaded Oral Hydrogel For Colon-Targeted Therapy In Inflammatory Bowel Disease. Int J Drug Deliv Technol. 2026;16(64s):965-983. DOI: 10.25258/ijddt.16.64s.94

INTRODUCTION

Inflammatory bowel disease (IBD), which includes Crohn's disease and ulcerative colitis, is one of the most important chronic gastrointestinal diseases around the world, affecting an estimated 6.8 million people worldwide and increasing in incidence from previously low prevalence regions such as Asia, the Middle-East and Latin America [1]. The disease has a significant economic impact, with costs in the U.S. alone in excess of $31 billion annually for direct health care costs and significant indirect costs due to lost productivity and diminished quality of life [2]. However, current pharmacological treatments, such as aminosalicylates, corticosteroids, immunomodulators and anti-tumor necrosis factor (TNF) biologics, often do not lead to sustained deep remission in a good number of patients [3]. Biological therapy fails in about 30% of patients, and fails in another 20–40% of those who responded initially to biological therapy [4]. Long-term

immunosuppressive therapy also poses serious infection risk, lymphoma risk, and risk of steroid toxicity. This is because systemic anti-inflammatory agents achieve poor colonic drug concentrations and can be associated with systemic side effects, creating an unmet need for colonic drug delivery platforms that can deliver therapeutic agents directly to the site of intestinal inflammation [5].

The anti-inflammatory, antioxidant and immunomodulatory properties of a natural flavonoid glycoside, baicalin, isolated from the root of *Scutellaria baicalensis* Georgi, make it a pharmacologically interesting compound for the treatment of IBD [6]. The main therapeutic mechanisms of action of baicalin involve the inhibition of the NFκB signaling pathway, the inhibition of proinflammatory cytokines such as tumor necrosis factor alpha, interleukin-1 beta and IL-6, the activation of the Nrf2-mediated antioxidant response, and the preservation of integrity of the intestinal epithelium by preserving the integrity of tight junction proteins [7]. Its efficacy has been consistently shown in dextran sulfate sodium-induced models of murine colitis, where it resulted in substantial attenuation of mucosal inflammation, protection of goblet cells through NLRP6 inflammasome activation, and favourable modulation of the gut microbiota composition [8]. Although this is an attractive profile of properties, baicalin is a drug considered to be very poorly soluble in water, with an apparent aqueous solubility of only 0.069 mg/mL, and is poorly absorbed in the intestine, while also being extensively metabolized in the liver [9]. The inherent biopharmaceutical properties lead to sub-therapeutic levels of drug at the inflamed colonic mucosa after a conventional oral dose limiting its clinical use [10].

Poly lactic-co-glycolic acid (PLGA) polymeric nanoparticles have been well established and FDA approved biodegradable platform that have various benefits for oral delivery, such as protecting the drug from gastrointestinal degradation, achieving controlled and sustained release of the drug, and facilitating enhanced mucosal absorption via endocytotic pathways with increased expression in the inflamed IBD epithelium [11]. Eudragit S100, a polymethacrylate copolymer that is soluble selectively in the colon (pH> 7.0), coating the nanoparticles impart pH responsive colon targeting whereby the drug is not released from the formulation until it reaches the colon [12]. The amphiphilic polyvinyl caprolactam-polyvinyl acetate-polyethylene glycol graft copolymer (Soluplus®) was examined as a solubilizer and stabilizer for BCS Class IV drugs, but its use as a colon targeted steric stabilizer in PLGA based nanoparticle systems for IBD has not been investigated [13]. Optimized nanoparticles are also incorporated into an oral hydrogel containing Carbopol 974NF to further enhance the colonic residence time, maintain the release of the nanoparticles at the mucosal surface and combine the complementary properties of nanoparticulate encapsulation and hydrogel-mediated mucosal retention [14].

The present study was designed to develop and optimize Baicalin loaded Eudragit S100 coated PLGA Nanoparticles using Soluplus® as a novel stabilizer using 3^2 full factorial design and to formulate optimized nanoparticles into oral hydrogel using Carbopol 974P NF and to evaluate the physicochemical properties, pH-responsive drug release, mucoadhesion, ex vivo colonic permeation and accelerated stability.

MATERIALS AND METHODS

MATRIALS

Baicalin (purity ≥98%, MW 446.36 g/mol) was procured from Sciquaint Innovations, Pune, India; PLGA (50:50, MW 30,000–60,000 Da) from Neeta Chemicals, Pune, India; Soluplus® (PVCap-PVAc-PEG graft copolymer) as a kind gift from BASF SE, Germany; and Eudragit S100 (methacrylic acid-methyl methacrylate, 1:2, dissolution pH ≥7.0) from Evonik Industries, Germany. Carbopol 974P NF (MW ~3,000,000 Da) was obtained from Lubrizol Corporation, USA. Glycerin, triethanolamine, acetone, isopropyl alcohol, sucrose (cryoprotectant grade), hydrochloric acid, sodium hydroxide, dimethyl sulphoxide, and ethanol were procured from Research Lab Fine Chem Industries, Mumbai, India. Potassium dihydrogen phosphate and disodium hydrogen phosphate were obtained from Neeta Chemicals, Pune, India. Dialysis membrane (MWCO 12–14 kDa) and membrane filters (0.45 µm) were supplied by HiMedia Laboratories Pvt. Ltd., Mumbai, India. Distilled water was prepared in-house. All other chemicals and reagents were of analytical grade.

METHODS

Calibration Curve of Baicalin

A calibration curve for baicalin was prepared in phosphate buffer saline (PBS, pH 7.4) to quantify the encapsulation efficiency, in vitro drug release studies and permeation studies. Baicalin was dissolved in a minimum amount of ethanol and then diluted to 100 mL with PBS pH 7.4 to make a stock solution (100 µg/mL). Solutions of 2, 4, 6, 8, 10 and 12 µg/mL of the working solutions were prepared by serial dilution. The absorbance was recorded at λmax 277 nm on UV-Visible double beam spectrophotometer LMSPUV1000B (LABMAN Scientific Instruments Pvt. Ltd., Tamil Nadu, India) with PBS pH 7.4 as blank. The absorbance of each sample was plotted against its concentration to

check for linearity, and regression equation and coefficient of determination (R^2) were calculated for drug quantification. Each measurement was made in triplicate (n = 3) [15,16].

Fourier Transform Infrared Spectroscopy

To evaluate the drug-excipient compatibility, FTIR spectroscopy was used to analyze the physical mixture of baicalin, PLGA, Soluplus®, Eudragit S100 and their chemical interactions. The samples were prepared by the KBr pellet method in which about 2 mg of each sample was mixed with dry KBr (spectroscopic grade) and pressed into transparent pellets with a hydraulic press. The spectra were recorded from 4000-400 cm-1 with a resolution of 4 cm-1 with Fourier Transform Infra Red (FTIR) Spectrometer (Spectrum One, Perk Elmer India Pvt. Ltd., India). Identification of characteristic absorption peaks and comparison of the obtained spectra with the reported reference spectra, to establish compatibility (n = 3) [17,18].

Differential Scanning Calorimetry

The thermal behavior and crystallinity of pure baicalin and physical mixture of baicalin with formulation excipients were evaluated by DSC analysis. About 5-8 mg of each sample was carefully placed into standard aluminium crimped pans, using an empty pan as a reference sample. The disappearance or shift of the characteristic endothermic peak of baicalin was considered as the sign of thermal incompatibility (n = 3) and was analyzed using a Differential Scanning Calorimeter (DSC 60 Plus, Shimadzu Analytical India Pvt. Ltd., Mumbai, India) under the N2 purge with heating rate of 10 °C/min from 30 to 300 °C [19,20].

Equilibrium Solubility Study

The equilibrium solubility of baicalin was determined in distilled water, 0.1 N HCl (pH 1.2), phosphate buffer (pH 6.8) and PBS (pH 7.4) to assist in selection of analytical media and release conditions. 10 mL of each medium was each placed in a sealed borosilicate glass tube and shaken at 100 rpm at 25 ± 1 °C for 72 hours on a rotary shaker (REMI Instruments Ltd., Mumbai, India), to which excess baicalin (~20 mg) was added. Samples were centrifuged for 15 minutes at 5000 rpm (Remi R-8C, Remi Electrotechnical Ltd., Mumbai, India), filtered through 0.45 µm membrane filters and analysed spectrophotometrically using the λmax 277 nm (Model LMSPUV1000B, LABMAN Scientific Instruments Pvt. Ltd., Tamilnadu, India). Solubility data were given as mean ± SD (n = 3) in mg/mL [21,22].

Experimental Design for Formulation Optimization

The effect of PLGA concentration (X_1) and Soluplus® concentration (X_2) on particle size (Y_1) and entrapment efficiency (Y_2) of baicalin loaded nanoparticles was investigated using 3^2 full factorial design. Three different levels were investigated for each factor, leading to nine formulation batches (NF1, NF2, NF3, NF4, NF5, NF6, NF7, NF8 and NF9). The model employed was the quadratic polynomial model which is: $Y = b_0 + b_1X_1 + b_2X_2 + b_{11}X_1^2 + b_{22}X_2^2 + b_{12}X_1X_2$ where b_0 is the intercept; b_1, b_2 are linear coefficients; b_{11}, b_{22} are quadratic coefficients; and b_{12} is the interaction coefficient. The desirability function approach of response surface analysis and optimization was carried out using Design-Expert® software (Version 13.0, USA, Stat-Ease Inc.) [23,24].

Table 1: Independent and Dependent Variables with Levels and Goals for 3^2 Factorial Design

Variable	Low (−1)	Medium (0)	High (+1)
Independent Variables			
X_1: PLGA Concentration (% w/v)	0.5	1.0	1.5
X_2: Soluplus® Concentration (% w/v)	0.5	1.0	1.5
Dependent Variables			**Goal**
Y_1: Particle Size (nm)			Minimize
Y_2: Entrapment Efficiency (%)			Maximize

Table 2: Formulation Table for 3^2 Factorial Design Batches of Baicalin-Loaded Polymeric Nanoparticles

Ingredient	NF1	NF2	NF3	NF4	NF5	NF6	NF7	NF8	NF9
Baicalin (mg)	10	10	10	10	10	10	10	10	10
PLGA (% w/v)	0.5	0.5	0.5	1.0	1.0	1.0	1.5	1.5	1.5
Soluplus® (% w/v)	0.5	1.0	1.5	0.5	1.0	1.5	0.5	1.0	1.5
Eudragit S100 (mg)	20	20	20	20	20	20	20	20	20
Acetone (mL)	5	5	5	5	5	5	5	5	5
Water q.s. to (mL)	25	25	25	25	25	25	25	25	25

Preparation of Baicalin-Loaded Polymeric Nanoparticles

The nanoprecipitation method was slightly modified to prepare baicalin loaded PLGA nanoparticles. Baicalin (10 mg) was co-dissolved with PLGA (batch specific concentration) in the organic phase (acetone, 5 mL) and stirred for 15 minutes at 500 rpm (REMI 2MLH, Remi Elektrotechnik Ltd, Mumbai, India). Soluplus® (batch specific concentration) was added to 25 mL of ultrapure water (aqueous phase) and shaken for 20 minutes at 400 rpm separately. The injection of the organic phase was performed dropwise in the aqueous phase using syringe pump at a rate of 1 mL/min while stirring at 800 rpm. Acetone was evaporated at 600 rpm, 40 ± 1 °C for 3 hours. Dissolved in acetone-isopropyl alcohol (1:1 v/v), Eudragit S100 (20 mg) was then added dropwise and stirred for 30 minutes to provide pH responsive colonic targeting. Dispersions were kept at 4 °C until characterized [25,26].

Characterization of Baicalin-Loaded Polymeric Nanoparticles

Particle Size, Polydispersity Index, and Zeta Potential

The dynamic light scattering and electrophoretic light scattering were used to measure the particle size and PDI, and zeta potential, respectively, of the dispersions of the nanoparticles. A diluent of 1:10 v/v of dispersions with filtered distilled water was analysed at 25 ± 1 °C with 173° scattering angle with Nano Particle Size Analyzer (Model PSAS1000, Microtrac MRB, India). Systems with PDI values less than 0.3 were deemed to be monodisperse. The results are given as mean ± SD (n = 3) [27].

Entrapment Efficiency and Drug Loading Capacity

The entrapment efficiency (EE%) and drug loading capacity (DL%) were calculated using ultrafiltration technique. For the preparation of the nanoparticle dispersion, two millilitre of the dispersion was centrifuged at 15,000 rpm for 30 minutes at 4 °C by Nanosep® centrifugal ultrafiltration tubes (MWCO 100 kDa). The filtrate was appropriately diluted with PBS, pH 7.4, and the amount of free baicalin was spectrophotometrically quantified at λmax 277 nm (Model LMSPUV1000B, LABMAN Scientific Instruments Pvt. Ltd., TamilNadu, India). The values of EE% and DL% were estimated as follows:

EE (%) = [(Total drug added − Free drug) / Total drug added] × 100

DL (%) = (Total drug added – Free drug / Total weight of the nanoparticles) × 100

The data have been presented as mean ± SD (n = 3) [28].

Surface Morphology

Optimized nanoparticles were characterized with scanning electron microscopy (SEM) for their surface morphology. The diluted dispersion of nanoparticles was dropped onto a carbon coated stub, allowed to air dry and then sputter coated with gold-palladium for 120 seconds in vacuum. The samples were studied under the Scanning Electron Microscope (EVO MA 10, Carl Zeiss India Pvt. Ltd. Bangalore, India) with an accelerating voltage of 10–15 kV [29].

In Vitro Drug Release Study

The pH-responsive drug release from nanoparticles was studied by dialysis bag diffusion method. The loaded dialysis bags (MWCO 12–14 kDa, HiMedia Laboratories Pvt. Ltd., Mumbai, India) were placed sequentially in 0.1 N HCl (pH 1.2, 2 hours), PBS pH 6.8 (2 hours) and PBS pH 7.4 (8 hours) in a water bath shaker (Navyug Scientific Instruments, New Delhi, India) at 37 ± 0.5 °C, 100 rpm. The sample was taken at 0, 1, 2, 4, 6, 8, 10 and 12 hours and 3 mL of medium was immediately replaced with the same amount of new medium to keep up sink conditions. The samples were filtered through membrane filters of 0.45 µm and analyzed using Model LMSPUV1000B, LABMAN Scientific Instruments Pvt. Ltd., Tamilnadu, India at the maximum absorbance of 277 nm. One-way ANOVA followed by Tukey's post-hoc test ($p < 0.05$) was used for statistical analysis. Data are presented as mean ± SD (n = 3) [30].

Drug Release Kinetics

The cumulative release data was fitted to four models including zero-order, first order, Higuchi, Hixson-Crowell and Korsmeyer-Peppas models to determine the drug release mechanism. The Korsmeyer-Peppas model was written as:

$Q/Q\infty = Ktn$

Here, $Q/Q\infty$ is the fraction of drug released at time t, K is the kinetic constant and n is the release exponent. For $n \leq 0.43$, anomalous transport takes place, for $0.43 < n < 0.85$, Fickian diffusion occurs, and for $n \geq 0.85$, Case II transport occurs. The model which had the highest R^2 was taken as the best fit [31].

Percentage Yield

The lyophilized amount of the lyophilized dispersion of nanoparticles in pre-weighed petri dishes (Labconco FreeZone, Labconco Corp., USA) to constant weight was used to calculate the percentage yield. The yield was defined as:

% Yield = (Actual yield / Theoretical yield) x 100

Data are presented as mean ± SD (n = 3) [32].

Preparation of Baicalin Nanoparticle-Loaded Oral Hydrogel

An oral hydro gel loaded with Baicalin nanoparticles was prepared.An oral hydro gel loaded with Baicalin nanoparticles was prepared. Carbopol 974P NF (0.5- 2.0 % w/w) was dispersed into 80% of total water volume under stirring at 500 rpm in 30 mins at room temp. The optimized nanoparticle dispersion (i.e., 1% w/w baicalin) was then added dropwise with continuous stirring at 300 rpm and then, glycerin (5% w/w) was added as a humectant. The gelation was carried out by dropwise addition of triethanolamine to neutralise and gel the solution to pH 6.8 ± 0.2. The volume was made up to 20 g using distilled water. Four batches, G1-G4, with different concentrations of Carbopol 974P NF (0.5, 1.0, 1.5 and 2.0 % w/w), were prepared and stored in amber glass containers for 24 hours before characterization [33,34].

Table 3: Formulation Composition of Baicalin Nanoparticle-Loaded Oral Hydrogel Batches (Batch Size: 20 g)

Ingredient	G1	G2	G3	G4
Baicalin Concentration in Gel (% w/w)	1%	1%	1%	1%
Carbopol 974P NF (% w/w)	0.5	1.0	1.5	2.0
Glycerin (% w/w)	5.0	5.0	5.0	5.0
Triethanolamine (q.s. to pH 6.8)	q.s.	q.s.	q.s.	q.s.
Distilled Water q.s. to (g)	20	20	20	20

Characterization of Baicalin Nanoparticle-Loaded Oral Hydrogel

Physical Appearance and pH

Color, clarity, homogeneity and consistency were visually inspected for the hydrogel batches. The pH was determined by dilution of 1 g of gel in 10 mL of distilled water and read at 25 ± 1 °C using a digital pH meter (LABMAN Scientific Instruments Pvt. Ltd., Tamilnadu, India) and the results were expressed as mean ± SD (n = 3) [35].

Viscosity

The viscosity of hydrogel batches was determined at 25 ± 1 °C under shear rates of 5, 10, 20, 30 and 50 rpm, using a Brookfield Rotational Viscometer (Model DV-E, Brookfield Engineering Laboratories Inc., USA) with spindle no. 7. Viscosity was depicted as a function of spindle speed to obtain a rheogram for characterisation of flow behaviour. Data presented as mean ± SD (n = 3) [36].

Spreadability

A parallel plate apparatus was used to measure the spreadability. Gel (0.5 g) was sandwiched between two glass plates under a 500 g load and the spread diameter was measured at one minute intervals for 5 minutes. Spreadability was worked out as:

$$S = m \times l / t$$

where m is the applied weight (g), l is the spread length (cm) and t is the time (s). The results are presented as mean ± SD (n = 3) [37].

Drug Content Uniformity

The gel equivalent (5 mg) was dissolved in PBS pH 7.4 and sonicated for 15 minutes, followed by centrifugation at 5000 rpm for 10 minutes and the supernatant was analyzed spectrophotometrically at the absorption peak λmax 277 nm using Model LMSPUV1000B (LABMAN Scientific Instruments Pvt. Ltd., TamilNadu, India). The mean ± SD (n = 3) values were reported as percentage of the labelled amount of the drugs [37].

Ex Vivo Mucoadhesive Strength

Ex vivo, the mucoadhesive strength was determined with freshly excised goat colonic mucosal tissue, which was obtained from a local abattoir and used within 2 hours of receiving the tissue. The mounted surface of mucosa was treated with gel (0.5 g) and left in contact for 5 minutes. The maximum detachment force (g) was obtained at a crosshead velocity of 0.5 mm/sec using a 0.5 N preload for 30 seconds. The values of mucoadhesive strength were presented in terms of maximum detachment force (g) and work of adhesion (g·sec) (n = 3, mean ± SD) [38].

Ex Vivo Permeation Study

A Franz diffusion cell assembly (LABMAN Scientific Instruments Pvt. Ltd., Tamilnadu, India) of 3.14 cm^2 diffusion area was used to evaluate the ex vivo permeation of baicalin through goat colonic mucosal membrane. The mucosal tissue was sandwiched between the donor and receptor chambers with the mucosal surface placed in the donor chamber filled with the same amount of gel equivalent to 5 mg of baicalin. PBS pH 7.4 was used in the receptor compartment at 37

± 0.5 °C, which was mechanically stirred at 100 rpm. Samples of 1 mL were taken at 0.5, 1, 2, 4, 6, 8 and 12 hours after which volume was replaced. Samples were analyzed at the λmax 277 nm and cumulative permeation (µg/cm²) was plotted as a function of time. Steady-state flux (Jss) was calculated as:Steady-state flux (Jss) was calculated as: Jss is the slope of the linear portion of the cumulative permeation vs. time graph

Kp = Jss / Cd

where Cd is the initial concentration of the donor. The results were reported as mean± SD (n = 3) [39].

Accelerated Stability Studies

The accelerated stability study was carried out at 40 ± 2 °C / 75 ± 5%RH in a programmable stability chamber (Remi Elektrotechnik Ltd., Mumbai, India) according to the ICH Q1A(R2) guidelines on the optimized batch of hydrogel formulation G3. Physical appearance, phase separation, pH, viscosity, drug content, entrapment efficiency and ex vivo cumulative permeation in 12 hours were determined at 0, 1, 2 and 3 months. Data were obtained in triplicate (n = 3) with the results presented as mean ± SD [40,41].

RESULTS AND DISCUSSION

RESULTS

Calibration Curve of Baicalin

The calibration curve of baicalin in PBS pH 7.4 showed good linearity and reproducibility between absorbance and concentration ranging from 2–12 µg/mL at λmax 277 nm (y = 0.0545x + 0.0042; R² = 0.9997) (Figure 1). The low value of the standard deviation in all concentrations confirmed the accuracy of the developed UV spectrophotometric method for further drug quantification studies.

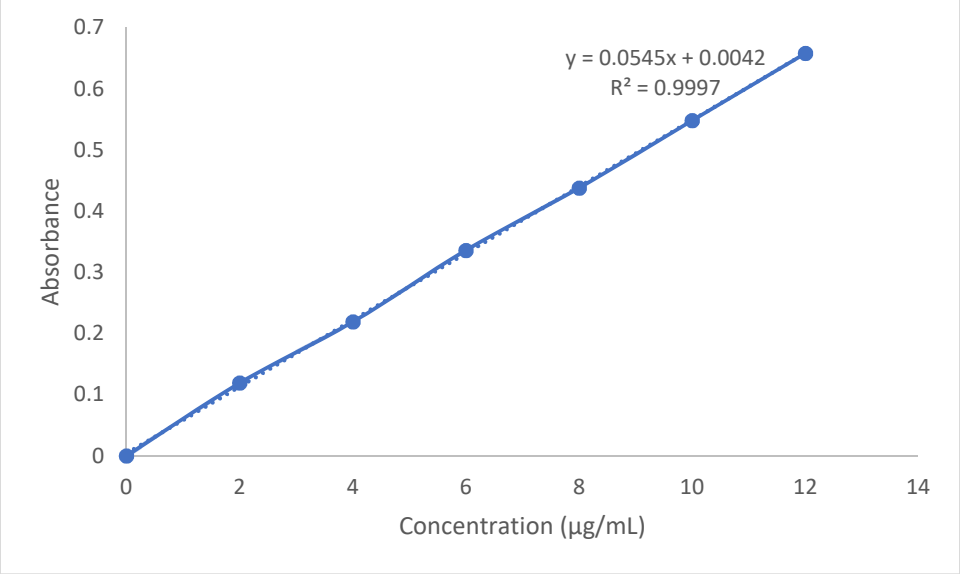

Figure 1: Calibration curve of baicalin in PBS pH 7.4 at λ_{max} 277 nm

Solubility Studies

The solubility of baicalin in different media was determined, and the results confirmed that the solubility was very low in distilled water (0.069 ± 0.003 mg/mL) and 0.1 N HCl (0.013 ± 0.001 mg/mL), while the solubility was markedly improved in PBS pH 6.8 (10.62 ± 0.38 mg/mL) and PBS pH 7.4 (12.18 ± 0.47 mg/mL), indicating that baicalin belongs to BCS Class IV (Table 4). The high pH sensitive solubility was the challenging factor which supported the development of the colon targeted delivery with PLGA nanoparticles coated with Eudragit S100.

Table 4: Equilibrium Solubility of Baicalin in Different Solvents and pH Media (25 ± 1 °C)

Sr. No.	Solvent / Medium	Solubility (mg/mL)	BCS Solubility Classification
1	Distilled Water	0.069 ± 0.003	Very Slightly Soluble
2	0.1 N HCl (pH 1.2)	0.013 ± 0.001	Very Slightly Soluble
3	PBS (pH 6.8)	10.62 ± 0.38	Sparingly Soluble
4	PBS (pH 7.4)	12.18 ± 0.47	Sparingly Soluble
5	Ethanol	3.84 ± 0.12	Slightly Soluble

6	DMSO	48.30 ± 1.24	Soluble

FTIR analysis

The O–H stretching and flavone carbonyl C=O (3384.61 cm-1 and 1721.86 cm-1, respectively) and glycosidic C–O–C linkages (1073.94, 1040.32 cm-1) were characteristic peaks of pure baicalin and were not significantly displaced in the physical mixture spectrum (Figure 2, Table 5). Superimposing peaks due to Eudragit S100 (1757.58 cm-1) and Soluplus® (1580.57 cm-1) indicated that there was no chemical incompatibility between each excipient in the formulation and baicalin.

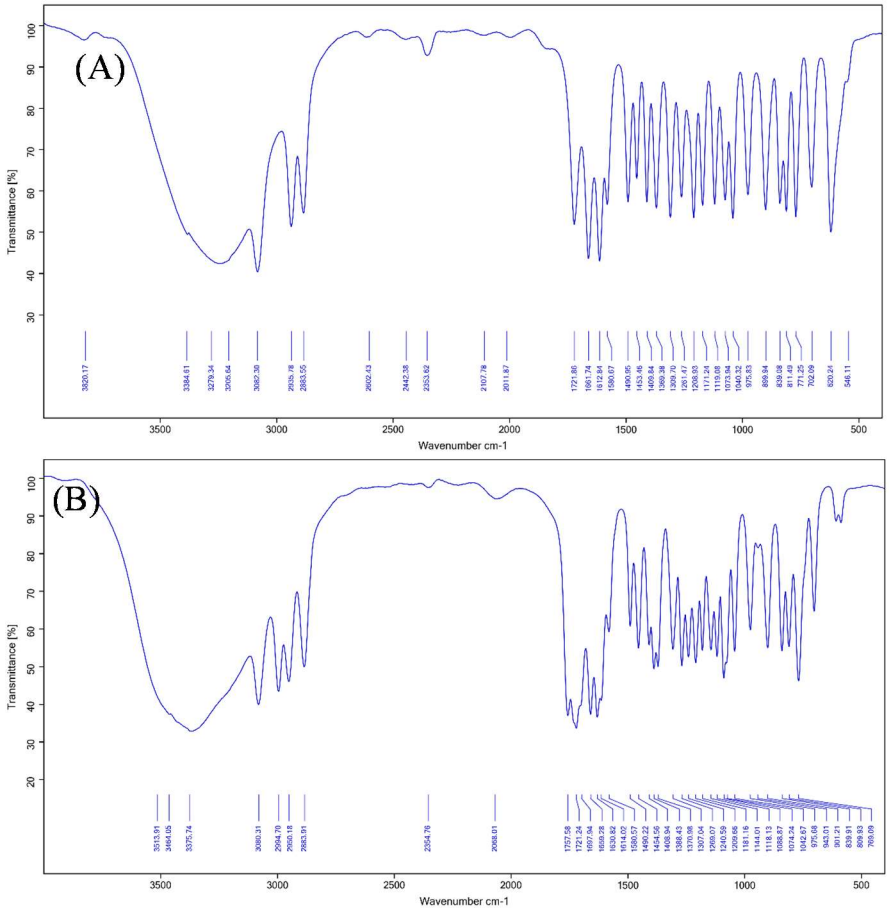

Figure 2: FTIR Spectra of (A) Pure drug and (B) Physical mixture

DSC analysis

The DSC thermogram of pure baicalin revealed a sharp endothermic melting peak at 196.49 °C, thus indicating the crystalline nature of the drug (Figure 3A). The thermal compatibility of baicalin with PLGA, Soluplus® and Eudragit S100 was confirmed by the presence of one peak of the characteristic melting temperature of the drug (196.53 °C) in combination with the appearance of another peak of PLGA transition (167.09 °C) in the physical mixture thermogram with no significant peak shifting or disappearance (Figure 3B), supporting the suitability of the selected excipient combination for nanoparticle formulation.

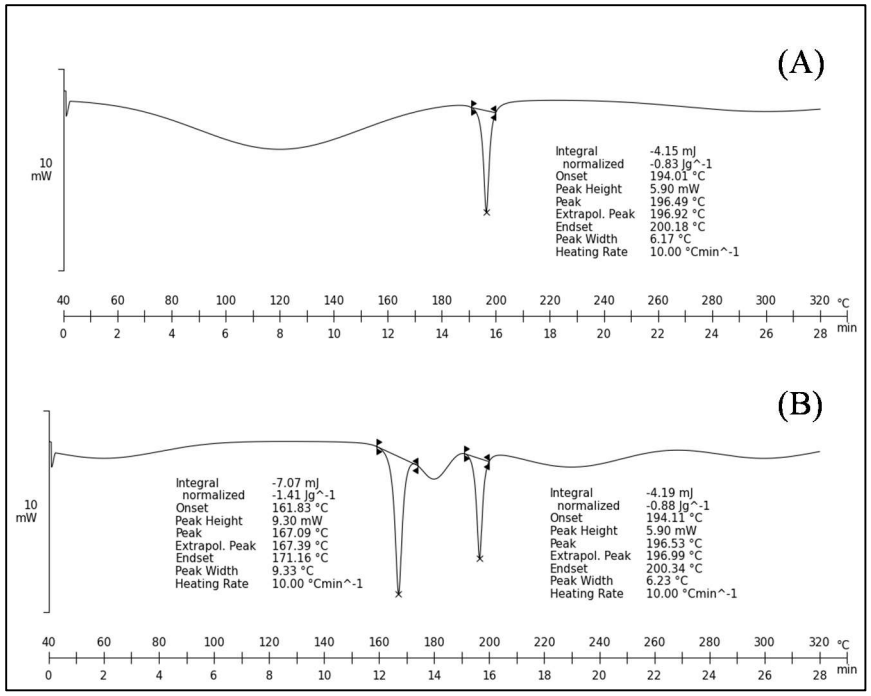

Figure 3: DSC Spectra of (A) pure drug and (B) Physical mixture

Characterization of Baicalin-Loaded Polymeric Nanoparticles

The nanoparticle batches NF1 – NF9 were characterized physicochemically, and the results are presented in Table 5 where the gradual increase of the PLGA and Soluplus® concentration in the batches was seen to increase all critical attributes. The decrease of particle size was from 312.4 ± 4.82 nm (NF1) to 176.2 ± 3.41 nm (NF9), PDI was decreased from 0.412 to 0.196, zeta potential was increased from −14.3 to −29.4 mV, and entrapment efficiency was improved from 61.3 ± 1.42% to 89.4 ± 1.08% for the factorial batches, all of which signify improved colloidal stability, better ability to encapsulate the drug, and formulation efficiency.

Table 5: Physicochemical Characterization of Baicalin-Loaded Polymeric Nanoparticles (NF1–NF9)

Batch	Particle Size (nm)	PDI	Zeta Potential (mV)	EE (%)	DL (%)	% Yield
NF1	312.4 ± 4.82	0.412 ± 0.018	-14.3 ± 0.74	61.3 ± 1.42	8.14 ± 0.38	71.2 ± 1.64
NF2	287.6 ± 3.97	0.374 ± 0.014	-16.8 ± 0.86	64.8 ± 1.18	8.62 ± 0.41	73.6 ± 1.48
NF3	268.1 ± 5.13	0.341 ± 0.021	-18.4 ± 0.91	67.2 ± 1.53	8.93 ± 0.34	74.8 ± 1.72
NF4	248.9 ± 4.36	0.318 ± 0.016	-19.7 ± 1.04	72.6 ± 1.37	9.64 ± 0.43	76.4 ± 1.53
NF5	224.3 ± 3.74	0.284 ± 0.012	-22.1 ± 0.88	77.4 ± 1.26	10.28 ± 0.37	79.3 ± 1.41
NF6	209.7 ± 4.21	0.261 ± 0.019	-24.3 ± 1.13	80.1 ± 1.44	10.64 ± 0.46	81.6 ± 1.58
NF7	198.4 ± 3.62	0.243 ± 0.013	-25.8 ± 0.97	82.3 ± 1.31	10.94 ± 0.39	83.2 ± 1.47
NF8	184.6 ± 4.08	0.218 ± 0.017	-27.6 ± 1.08	86.7 ± 1.19	11.52 ± 0.42	85.7 ± 1.62
NF9	176.2 ± 3.41	0.196 ± 0.011	-29.4 ± 0.83	89.4 ± 1.08	11.88 ± 0.36	87.4 ± 1.39

All data expressed in mean ± SD, (n=3).

In Vitro Drug Release Profile

All the batches of the nanoparticles (NF1 – NF9) showed pH responsiveness and sustained release profile when tested in the sequential pH media (Table 4). Cumulative release was not increased significantly at pH 1.2 and pH 6.8 below 14.26% at 4 hours, while above 12 hours, the amount of drug released increased, reaching 85.47 ± 1.72% for NF7 and 81.62 ± 1.58% for NF8, demonstrating satisfactory gastric protection and controlled colonic release of the drug by Eudragit S100.

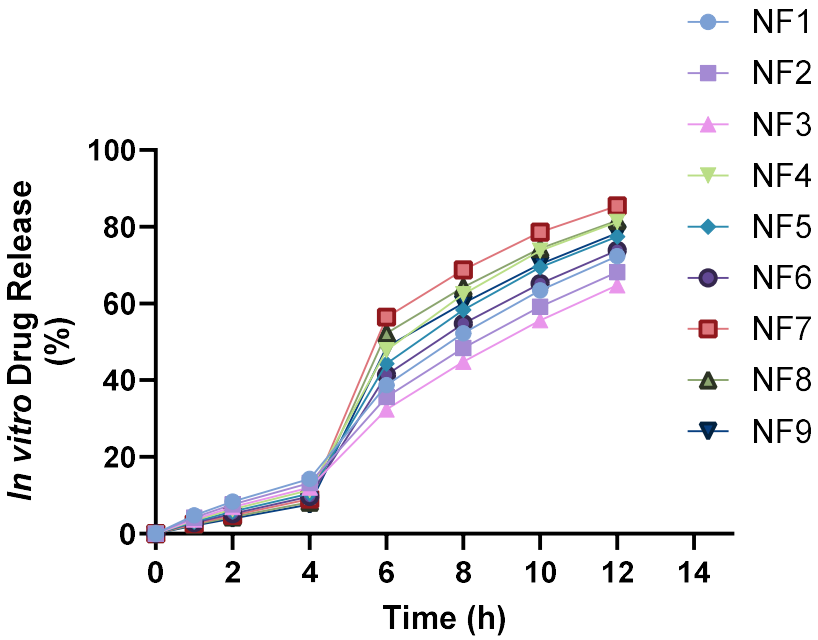

Table 4: *In Vitro* Drug Release Profile of Baicalin-Loaded Nanoparticles NF1–NF9 Across Sequential pH Media.

Optimization

Particle Size (Y1)

The quadratic model for particle size (Y1) proved to be highly significant ($F = 765.46$, $p < 0.0001$) and excellent fit statistics were obtained to ensure good predictability ($R^2 = 0.9992$, adjusted $R^2 = 0.9979$, predicted $R^2 = 0.9911$). The low coefficient of variation (0.9280%) and high adequate precision (77.7869) further confirmed the reliability of the model (Table 8.8, Table 8.9). PLGA concentration (A) exerted the most dominant effect on particle size ($F = 3358.85$, $p < 0.0001$), followed by Soluplus® concentration (B) ($F = 393.28$, $p = 0.0003$). The interaction term AB was significant ($F = 25.79$, $p = 0.0148$), and the quadratic term A^2 was also significant ($F = 44.38$, $p = 0.0069$), suggesting that the response was not linear, but rather curved. A regression equation for particle size was:

$$Y1 = 225.3333 - 51.4833A - 17.6167B + 5.525AB + 10.25A^2 + 3.45B^2$$

The negative values of A and B indicated that PLGA and Soluplus® concentrations increased proportionately to lower the particle size as they increased. The contour plot (Figure 8.8) showed elliptical contours which indicated a strong interaction between A and B and suggested that minimum particle size occurred at higher levels of both factors. As can be seen from the 3D response surface plot (Figure 8.9), the particle size decreased rapidly with increasing PLGA concentration while the Soluplus® concentration had a relatively mild impact over the experimental range.

Entrapment Efficiency (Y2)

The quadratic model of entrapment efficiency (Y2) was highly significant ($F = 1123.21$, $p < 0.0001$) and showed excellent agreement between the experimental values and the values predicted by the model, as evidenced by the high values of R^2 ($R^2 = 0.9995$), adjusted R^2 (adjusted $R^2 = 0.9986$), and predicted R^2 (predicted $R^2 = 0.9938$). The coefficient of variation (CV = 0.4926%) and adequate precision (AP = 93.6453) shows high precision of the model and reliability of the signal (Table 8.10, Table 8.11). The main factors affecting EE were the concentrations of PLGA (A) ($F = 5072.09$, $p < 0.0001$) and Soluplus® (B) ($F = 502.96$, $p = 0.0002$). No

interaction effect between the two factors was found (AB: p = 0.2062); however, significant curvature was found for the quadratic effect for A (A^2: p = 0.0127). The following regression equation was used to determine entrapment efficiency:

$$Y2 = 77.2444 + 10.85A + 3.4167B + 0.3AB - 1.4167A^2 - 0.8167B^2$$

The positive values of A and B indicated that the entrapment of baicalin in polymeric matrix improved with the increase in both PLGA and Soluplus® concentrations. As can be seen in the contour plot (Figure 8.12), the contour lines were near circular in shape, which supported the non-significant interaction between AB, with the highest level of entrapment occurring at high levels of both factors. The 3D response surface plot (Figure 8.13) showed a strong upward trend as the PLGA concentration increased, and a slight trend levelled off at higher concentrations due to the important negative quadratic term A^2.

Table 6: Fit Summary of Quadratic Models for Critical Quality Attributes of Baicalin-Loaded Polymeric Nanoparticles

Source	Sequential p-value	Lack of Fit p-value	Adjusted R^2	Predicted R^2	
Particle size					
Quadratic	0.0137		0.9979	0.9911	Suggested
Entrapment efficiency					
Quadratic	0.0195		0.9986	0.9938	Suggested

Table 7: ANOVA Summary for Quadratic Models of Particle Size (Y1) and Entrapment Efficiency (Y2) of Baicalin-Loaded Polymeric Nanoparticles

Source	Sum of Squares	df	Mean Square	F-value	p-value	Significance
Particle Size (Y1)						
Model	18121.32	5	3624.26	765.46	<0.0001	Significant
A: PLGA	15903.20	1	15903.20	3358.85	<0.0001	Significant
B: Soluplus®	1862.08	1	1862.08	393.28	0.0003	Significant
AB	122.10	1	122.10	25.79	0.0148	Significant
A^2	210.13	1	210.13	44.38	0.0069	Significant
B^2	23.81	1	23.81	5.03	0.1107	Not Significant
Residual	14.20	3	4.73	—	—	
Cor Total	18135.52	8	—	—	—	
Entrapment Efficiency (Y2)						
Model	782.08	5	156.42	1123.21	<0.0001	Significant
A: PLGA	706.33	1	706.33	5072.09	<0.0001	Significant
B: Soluplus®	70.04	1	70.04	502.96	0.0002	Significant
AB	0.3600	1	0.3600	2.59	0.2062	Not Significant
A^2	4.01	1	4.01	28.82	0.0127	Significant

B^2	1.33	1	1.33	9.58	0.0535	Not Significant
Residual	0.4178	3	0.1393	—	—	
Cor Total	782.50	8	—	—	—	

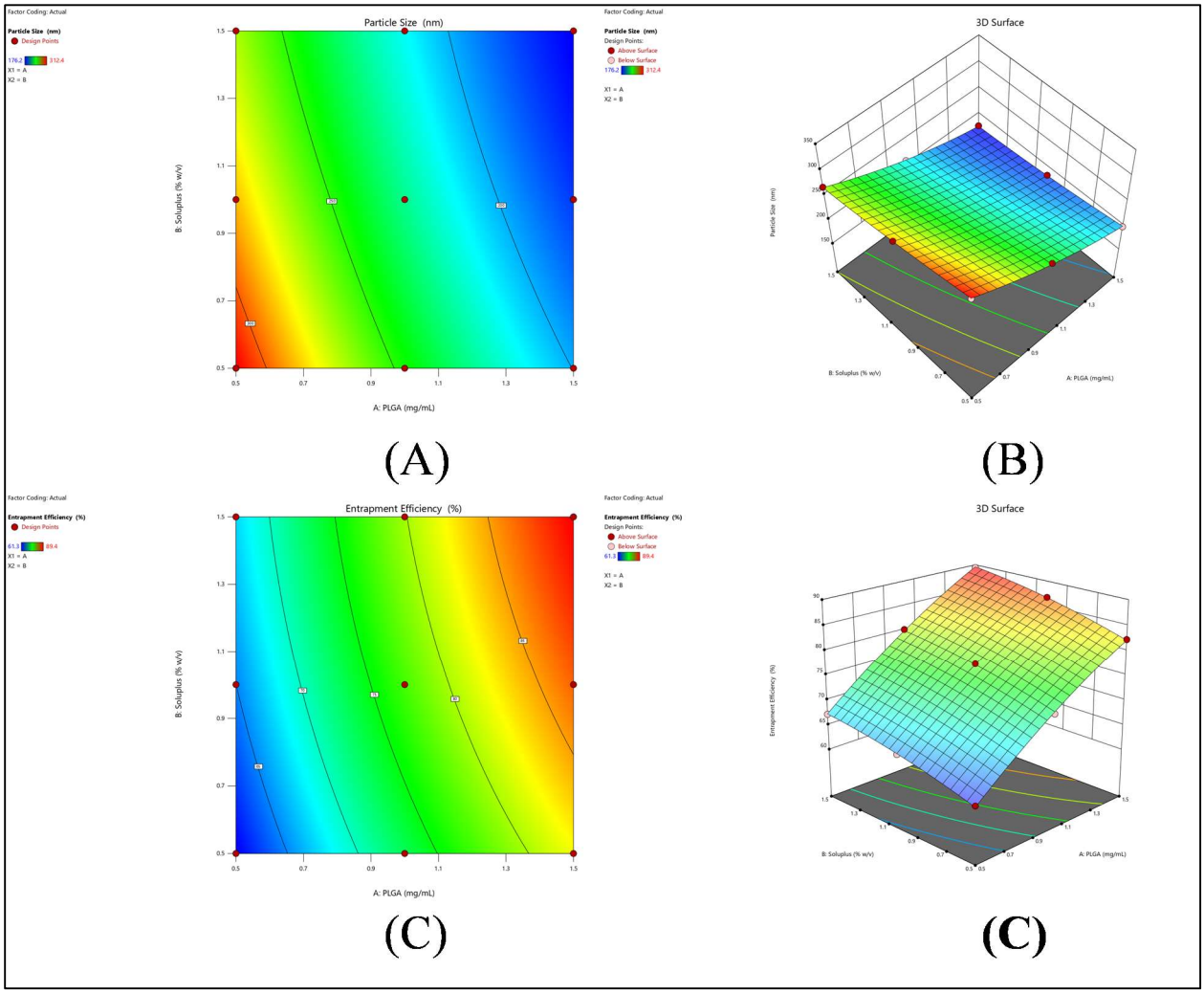

Figure 5: Effect of PLGA and Soluplus® concentrations on critical quality attributes of baicalin-loaded Eudragit S100-coated polymeric nanoparticles. (A) 2D contour plot and (B) response surface plot illustrating the combined influence of formulation variables on particle size (Y1); (C) 2D contour plot and (D) response surface plot illustrating the combined influence of formulation variables on entrapment efficiency (Y2).

The optimized batch NF8 (PLGA 1.5% w/v, Soluplus® 1.0% w/v) was validated where the experimental particle size (184.6 ± 4.08 nm) and EE (86.7 ± 1.19%) was comparable to the predicted particle size (184.1 nm) and EE (86.68%) with percentage relative errors of 0.27% and 0.02% respectively (Table 8). Both responses were successfully optimized with a desirability score of 1.000.

Validation of statistical models

Table 8: Validation of Optimized Batch (NF8) by Comparison of Predicted and Experimental Values

Response	PLGA (% w/v)	Soluplus® (% w/v)	Predicted Value	Experimental Value	% Relative Error	Desirability

Particle Size (nm)	1.5	1.0	184.1	184.6 ± 4.08	0.27	1.000
Entrapment Efficiency (%)	1.5	1.0	86.68	86.7 ± 1.19	0.02	1.000

Drug release kinetic

The best fit for drug release data of optimized batch NF8 was the first-order model (R^2 = 0.9507), which suggested that the release of the drug was concentration-dependent from the PLGA nanoparticle matrix (Figure 6). Case II transport with polymer relaxation and Eudragit S100's erosion was considered to be the dominant release mechanism as the Korsmeyer-Peppas release exponent (n = 1.6012) was more than 0.85, which is the threshold value for Case II transport. The Higuchi R^2 value of 0.8282 was lower than the threshold value for Case II transport (n > 0.85), and this result also confirmed that pure Fickian diffusion was not the dominant release mechanism.

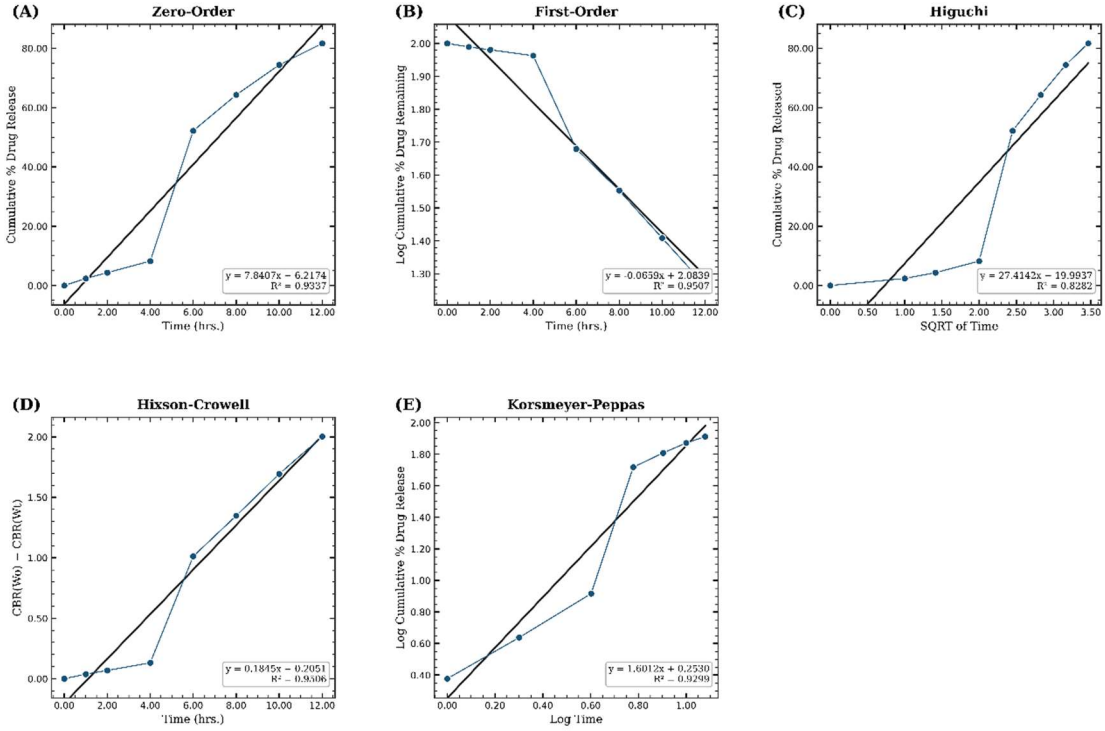

Figure 6: Drug release kinetic plots of optimized baicalin nanoparticle batch NF8 fitted to (A) Zero-order, (B) First-order, (C) Higuchi, (D) Hixson-Crowell, and (E) Korsmeyer-Peppas models.

TEM analysis

The optimized batch NF8 was analyzed by TEM and showed the presence of well-defined spherical nanoparticles with a clear core-shell structure, where the electron dense PLGA core was clearly coated with an electron light coating layer of Eudragit S100 (Figure 7). The particle size measured by TEM was consistent with the DLS measurement result (184.6 nm), which shows particle size measurement reliability. The uniformity in the size distribution and discrete and distinct particle morphology in the micrograph was supported by the low PDI of 0.218.

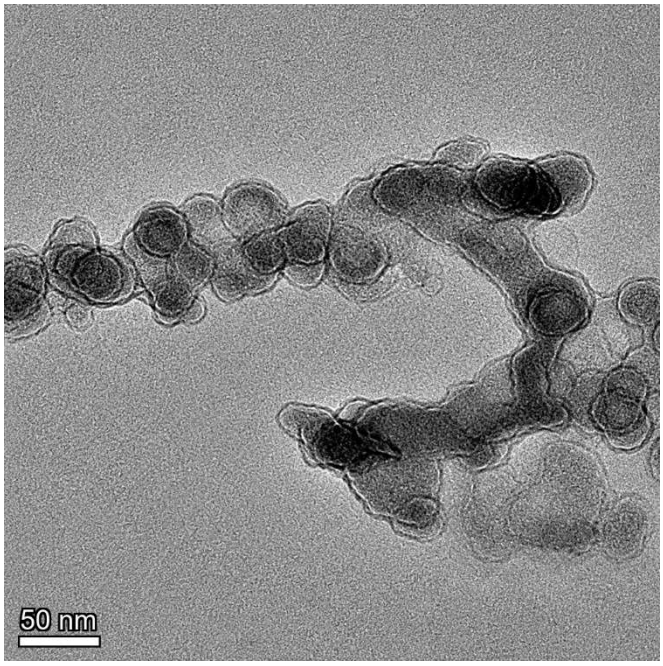

Figure 7: Transmission electron micrograph of optimized baicalin-loaded polymeric nanoparticle batch NF8 showing spherical morphology with distinct core-shell architecture (scale bar = 50 nm).

Characterization of Optimized Baicalin Nanoparticle-Loaded Oral Hydrogel

All the batches G1–G4 had a pH range between 6.74 ± 0.06 to 6.86 ± 0.07, which was close to the physiological oral pH, and the appearance was pale yellow, translucent and homogeneous with no phase separation (Table 9). The viscosity of the formulations also showed a gradual increase from 1248.4 ± 38.6 cP (G1) to 12683.4 ± 96.7 cP (G4) with the increase in the concentration of Carbopol 974P NF; the spreadability showed a gradual decrease from 18.42 ± 0.74 to 7.24 ± 0.47 g·cm/sec with increase in batch concentration and the drug content remained constant across all batches (98.42–99.13%).

Table 9: Physical appearance and pH of baicalin nanoparticle-loaded oral hydrogel batches G1–G4

Parameter	G1	G2	G3	G4
Appearance	Translucent, slightly fluid	Translucent, semi-solid	Translucent, smooth gel	Translucent, stiff gel
Colour	Pale yellow	Pale yellow	Pale yellow	Pale yellow
Homogeneity	Homogeneous	Homogeneous	Homogeneous	Homogeneous
Phase Separation	Absent	Absent	Absent	Absent
pH	6.74 ± 0.06	6.81 ± 0.04	6.83 ± 0.05	6.86 ± 0.07

All data expressed in mean ± SD, (n=3).

Table 10: Viscosity, Spreadability, and Drug Content of Hydrogel Batches G1–G4

Parameter	G1	G2	G3	G4
Viscosity at 50 rpm (cP,)	1248.4 ± 38.6	3874.2 ± 52.4	7436.8 ± 74.3	12683.4 ± 96.7
Spreadability (g·cm/sec,)	18.42 ± 0.74	14.67 ± 0.58	10.83 ± 0.63	7.24 ± 0.47
Drug Content (% w/w)	98.42 ± 0.84	98.87 ± 0.72	99.13 ± 0.68	99.04 ± 0.76

All data expressed in mean ± SD, (n=3).

***Ex vivo* mucoadhesive strength**

The mucoadhesive strength parameters on ex vivo samples also showed the increase with the increase in the concentration of Carbopol 974P NF (Table 11). The progressive increase in polymer–mucin interactions is to be expected as the concentration of Carbopol increases, resulting in greater mucoadhesion residence time (from 38.4 ± 2.1 to 81.3 ± 2.7 minutes), work of adhesion (from 24.17 ± 1.14 to 79.34 ± 1.67 g·sec), and maximum detachment force (from 8.34 ± 0.42 g (G1) to 26.87 ± 0.71 g (G4)).

Table 11: *Ex vivo* mucoadhesive strength parameters of baicalin nanoparticle-loaded oral hydrogel batches G1-G4 on goat colonic mucosal tissue

Parameter	G1	G2	G3	G4
Maximum Detachment Force (g)	8.34 ± 0.42	14.76 ± 0.58	21.43 ± 0.64	26.87 ± 0.71
Work of Adhesion (g·sec)	24.17 ± 1.14	43.62 ± 1.38	64.28 ± 1.52	79.34 ± 1.67
Mucoadhesion Residence Time (min)	38.4 ± 2.1	54.7 ± 1.8	72.6 ± 2.4	81.3 ± 2.7

All data expressed in mean ± SD, (n=3).

Ex Vivo Cumulative Drug Permeation

The cumulative drug permeation was found to be in the following order: G3 > G2 > G1 > G4; the highest cumulative permeation by G3 was 68.24 ± 1.36% with steady state flux of 107.44 µg/cm²/hr and permeability coefficient of 0.02149 cm/hr after 12 hrs (Figure 8 and Table 12). G3 was found to be the optimal hydrogel batch in terms of the balance between mucoadhesion, viscosity and permeation and G4 showed the lowest permeation (54.17 ± 1.24%) due to the excessive gel stiffness restricting the drug diffusion.

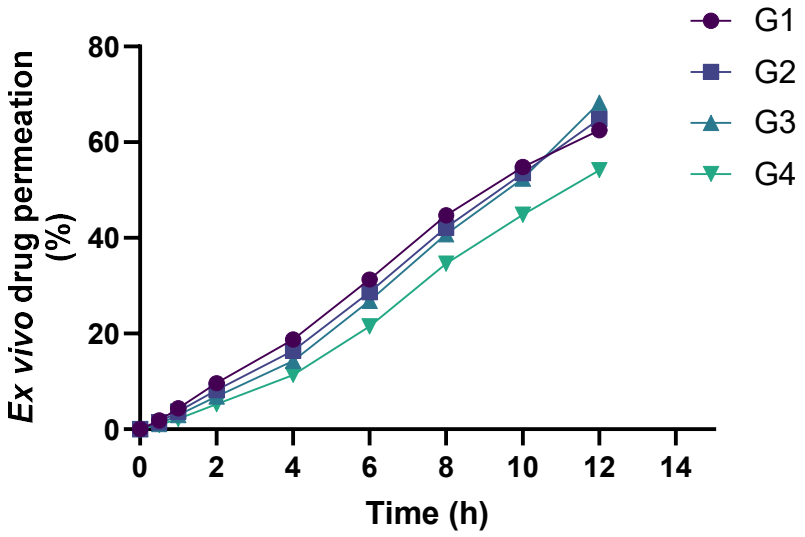

Figure 8: *Ex Vivo* Cumulative Drug Permeation (%) Through Goat Colonic Mucosal Membrane from Hydrogel Batches G1-G4

Table 12: Steady-State Flux and Permeability Coefficient of Baicalin from Hydrogel Batches G1-G4 Through Goat Colonic Mucosal Membrane

Batch	Carbopol 974P NF (% w/w)	Steady-State Flux Jss (µg/cm²/hr)	Permeability Coefficient Kp (cm/hr)
G1	0.5	87.00	0.01740
G2	1.0	96.38	0.01928
G3	1.5	107.44	0.02149
G4	2.0	85.23	0.01705

Accelerated Stability Studies

The robustness of the formulation was checked in accelerated stability studies for three months at 40 °C ± 2 °C, 75 %RH, followed by G3 formulation (Table 13), which showed no phase separation and retained the pale yellow, translucent and homogeneous appearance of the product throughout the study. Minor variations were observed in pH (6.83 to 6.77), viscosity (7436.8 to 7361.3 cP), drug content (99.13 to 98.52%), entrapment efficiency (86.7 to 85.8%), and 12-hour ex vivo permeation (68.24 to 67.27%), all remaining within acceptable limits as per ICH Q1A(R2) guidelines.

Table 13: Accelerated stability profile of optimized baicalin nanoparticle-loaded oral hydrogel batch G3 stored at 40 ± 2 °C / 75 ± 5% RH for three months as per ICH Q1A(R2) guidelines

Parameter	0 Month	1 Month	2 Months	3 Months
Physical Appearance	Pale yellow, translucent, homogeneous gel	Pale yellow, translucent, homogeneous gel	Pale yellow, translucent, homogeneous gel	Pale yellow, translucent, homogeneous gel
Phase Separation	Absent	Absent	Absent	Absent
pH	6.83 ± 0.05	6.81 ± 0.04	6.79 ± 0.06	6.77 ± 0.05
Viscosity at 50 rpm (cP)	7436.8 ± 74.3	7412.4 ± 68.7	7384.6 ± 71.2	7361.3 ± 66.8
Drug Content (%)	99.13 ± 0.68	98.94 ± 0.62	98.76 ± 0.71	98.52 ± 0.64
Entrapment Efficiency (%)	86.7 ± 1.19	86.4 ± 1.14	86.1 ± 1.21	85.8 ± 1.16
Ex Vivo Cumulative Drug Permeation at 12 hr (%)	68.24 ± 1.36	67.94 ± 1.28	67.61 ± 1.34	67.27 ± 1.31

All data expressed in mean ± SD, (n=3).

DISCUSSION

The present study was successful in the development of baicalin loaded Eudragit S100 coated PLGA nanoparticles stabilized with Soluplus®, which were incorporated into the oral hydrogel made from Carbopol 974P NF for colon targeted anti-inflammatory drug delivery systems for IBD [42]. The preformulation studies revealed that baicalin belongs to BCS Class IV, as its solubility in water (0.069 mg/mL) was significantly improved in the case of pH 7.4 (Table 4), which is consistent with its previously reported pH-dependent solubility characteristics of flavonoid glycosides [43]. FTIR (Figure 2) and DSC (Figure 3) analyses showed that there was no interaction between baicalin and all excipients in the physical mixtures and the characteristic endothermic peak of baicalin at 196.53 °C was maintained, similar to the report of Riadi et al. on the physical and chemical compatibility of baicalin with lipid and polymer components in lipid-polymer hybrid nanoparticles [44]. According to ANOVA (Table 7), the quadratic model was found to be excellent in predicting both particle size (R^2 = 0.9992, F = 3358.85) and entrapment efficiency (R^2 = 0.9995, F = 5072.09) and the PLGA concentration was which had the greatest influence. Optimized batch NF8 (184.6 nm, PDI 0.218, zeta potential of −27.6 mV, and entrapment efficiency of 86.7%) was comparable with the particle size (184.3 nm) and satisfactory encapsulation (86.7%) reported by Riadi et al. on similar PLGA-based baicalin nanoparticles [45].

The pH-responsive in vitro release profile showed that the drug release was minimal below 81.62% at pH 1.2 and 6.8, and sustained release in the colon at 12 hours for NF8, which proved that the Eudragit S100 coating provided a sufficient gastric protection, in accordance with the findings by Huang et al. that the Eudragit S100 coating completely suppressed the release of baicalin in gastric and intestinal media [46]. Thefirst order release kinetics with Korsmeyer-Peppas n = 1.6012 (Figure 6) were identified, which suggested Case II transport, which was related to the relaxation of the polymer, and supported the erosion-controlled release mechanism reported for Eudragit-coated polymeric nanoparticulate systems [47]. The concentration-dependent physicochemical behavior of the incorporation of optimized nanoparticles into Carbopol 974P NF hydrogel, performed in the different batches (G1-G4), showed that as the concentration of the polymer increased, the viscosity of the resulting hydrogel increased from 1248.4 to 12683.4 cP, which is consistent with the increasing polymer concentration and the progressive strengthening of the gel network, as reported by Wu et al. for mucoadhesive colitis-targeted hydrogels, and the spreadability of the hydrogels

decreased inversely from 18.42 to 7.24 g·cm/sec (Table 10) [48]. The drug content uniformity was also high in all the batches, ranging from 98.42 to 99.13%, which shows the uniform distribution of nanoparticles in the gel matrix. G3 showed highest cumulative permeation (68.24%) after 12 hours, along with the highest steady state flux (107.44 µg/cm²/hr) and permeation coefficient (0.02149 cm/hr) with the incremental increase in the polymer concentration the ex vivo mucoadhesive strength parameters were increased in a progressive manner from G1 to G4 (Table 11) and the highest detachment force (26.87 g), work of adhesion (79.34 g·sec) was not obtained at the higher polymer concentration [49]. This result is consistent with the results of Wang et al. who also found a critical polymer concentration for the delivery of magnolol in core-shell nanoparticle-hydrogel microsphere systems for ulcerative colitis; too much gel stiffness prevented drug permeation. The nano-in-hydrogel structure used in the present study is similar to the nano-in-micro structure introduced by Zhang et al. for curcumin colonic delivery, which involved the use of a hydrogel matrix to extend the residence time of the nanoparticles in the colon and use the nanoparticles to promote penetration of the mucosa. The optimized batch G3 was found to be stable at accelerated conditions of three months at 40 ± 2 °C / 75 ± 5% RH, where all critical parameters such as drug content (99.13 to 98.52%), entrapment efficiency (86.7 to 85.8%), and ex vivo permeation after 12 h (68.24 to 67.27%) were within acceptable limits (Table 13), indicating the developed baicalin nanoparticle loaded oral hydrogel as a stable, pH responsive, mucoadhesive colon targeted platform with high translational potential for IBD therapy till in vivo pharmacodynamic study [50].

CONCLUSION

In the present work, a novel pH-responsive colon targeted delivery system with optimized baicalin loaded Eudragit S100-coated PLGA nanoparticles stabilized with a novel steric stabilizer Soluplus® to be used in pH-responsive oral hydrogel for the delivery of baicalin in inflammatory bowel diseases succeeded. The optimized batch NF8 had good physicochemical properties, such as particle size of 184.6 nm, entrapment efficiency of 86.7% and sustained colonic drug release of 81.62% at 12 hours, while the optimized batch G3 had excellent mucoadhesion properties, optimal spreadability and highest cumulative permeation in ex vivo of 68.24% with steady state flux of 107.44 µg/cm²/hr. Formulation robustness has been confirmed by accelerated stability studies for 3-months under the ICH Q1A(R2) conditions. The developed system has significant clinical benefits such as increasing the local anti-inflammatory drug concentration at the inflamed colonic mucosa, decreasing systemic drug exposure, and patient compliance of the oral route. Future studies in relevant animal models of colitis would be useful to validate the therapeutic efficacy and applicability of the developed platform in vivo; in vivo PKP would help support this.

ABBREVIATIONS

IBD: Inflammatory Bowel Disease; PLGA: Poly Lactic-co-Glycolic Acid; BCS: Biopharmaceutical Classification System; FTIR: Fourier Transform Infrared Spectroscopy; DSC: Differential Scanning Calorimetry; PDI: Polydispersity Index; EE: Entrapment Efficiency; DL: Drug Loading; TEM: Transmission Electron Microscopy; PBS: Phosphate Buffer Saline; NF-κB: Nuclear Factor Kappa B; TNF-α: Tumor Necrosis Factor Alpha; UV-Vis: Ultraviolet-Visible Spectrophotometry; ANOVA: Analysis of Variance; ICH: International Council for Harmonisation; RH: Relative Humidity; Jss: Steady-State Flux; Kp: Permeability Coefficient; RPM: Revolutions Per Minute; SD: Standard Deviation; R^2: Coefficient of Determination; df: Degree of Freedom; CV: Coefficient of Variation; w/v: Weight per Volume; w/w: Weight per Weight.

REFERENCES

[1] Neurath MF. Strategies for targeting cytokines in inflammatory bowel disease. Nat Rev Immunol 2024;24:559–76. https://doi.org/10.1038/s41577-024-01008-6.

[2] El Hadad J, Schreiner P, Vavricka SR, Greuter T. The Genetics of Inflammatory Bowel Disease. Mol Diagn Ther 2024;28:27–35. https://doi.org/10.1007/s40291-023-00678-7.

[3] Ashton JJ, Beattie RM. Inflammatory bowel disease: recent developments. Arch Dis Child 2024;109:370–6. https://doi.org/10.1136/archdischild-2023-325668.

[4] McDowell C, Farooq U, Haseeb M. Inflammatory Bowel Disease. StatPearls Internet, StatPearls Publishing; 2023.

[5] Liu Z, Liu R, Gao H, Jung S, Gao X, Sun R, et al. Genetic architecture of the inflammatory bowel diseases across East Asian and European ancestries. Nat Genet 2023;55:796–806. https://doi.org/10.1038/s41588-023-01384-0.

[6] Wen Y, Wang Y, Zhao C, Zhao B, Wang J. The Pharmacological Efficacy of Baicalin in Inflammatory Diseases. Int J Mol Sci 2023;24:9317. https://doi.org/10.3390/ijms24119317.

[7] Qiu X, Huang R, Xie J, Luo S, Cheng X, Cui J, et al. Recent Advances in the Therapeutic Effects and Molecular Mechanisms of Baicalin. Biology

2025;14:637. https://doi.org/10.3390/biology14060637.

[8] Bao M, Ma Y, Liang M, Sun X, Ju X, Yong Y, et al. Research progress on pharmacological effects and new dosage forms of baicalin. Vet Med Sci 2022;8:2773–84. https://doi.org/10.1002/vms3.960.

[9] Hu Z, Guan Y, Hu W, Xu Z, Ishfaq M. An overview of pharmacological activities of baicalin and its aglycone baicalein: New insights into molecular mechanisms and signaling pathways. Iran J Basic Med Sci 2022;25:14–26. https://doi.org/10.22038/IJBMS.2022.60380.13381.

[10] Ganguly R, Gupta A, Pandey AK. Role of baicalin as a potential therapeutic agent in hepatobiliary and gastrointestinal disorders: A review. World J Gastroenterol 2022;28:3047–62. https://doi.org/10.3748/wjg.v28.i26.3047.

[11] Shakya AK, Al-Sulaibi M, Naik RR, Nsairat H, Suboh S, Abulaila A. Review on PLGA Polymer Based Nanoparticles with Antimicrobial Properties and Their Application in Various Medical Conditions or Infections. Polymers 2023;15:3597. https://doi.org/10.3390/polym15173597.

[12] Vallorz EL, Encinas-Basurto D, Schnellmann RG, Mansour HM. Design, Development, Physicochemical Characterization, and In Vitro Drug Release of Formoterol PEGylated PLGA Polymeric Nanoparticles. Pharmaceutics 2022;14:638. https://doi.org/10.3390/pharmaceutics14030638.

[13] Sharifyrad M, Gohari S, Fathi M, Danafar H, Hosseini M-J, Mostafavi H, et al. The efficacy and neuroprotective effects of edaravone-loaded mPEG-b-PLGA polymeric nanoparticles on human neuroblastoma SH-SY5Y cell line as in vitro model of ischemia. J Drug Deliv Sci Technol 2022;73:103378. https://doi.org/10.1016/j.jddst.2022.103378.

[14] Pinto M, Silva V, Barreiro S, Silva R, Remião F, Borges F, et al. Brain drug delivery and neurodegenerative diseases: Polymeric PLGA-based nanoparticles as a forefront platform. Ageing Res Rev 2022;79:101658. https://doi.org/10.1016/j.arr.2022.101658.

[15] Chatterjee M, Chanda N. Formulation of PLGA nano-carriers: specialized modification for cancer therapeutic applications. Mater Adv 2022;3:837–58. https://doi.org/10.1039/D1MA00600B.

[16] Sakhi M, Khan A, Iqbal Z, Khan I, Raza A, Ullah A, et al. Design and Characterization of Paclitaxel-Loaded Polymeric Nanoparticles Decorated With Trastuzumab for the Effective Treatment of Breast Cancer. Front Pharmacol 2022;13. https://doi.org/10.3389/fphar.2022.855294.

[17] Almoustafa HA, Alshawsh MA, Al-Suede FSR, Alshehade SA, Abdul Majid AMS, Chik Z. The Chemotherapeutic Efficacy of Hyaluronic Acid Coated Polymeric Nanoparticles against Breast Cancer Metastasis in Female NCr-Nu/Nu Nude Mice. Polymers 2023;15:284. https://doi.org/10.3390/polym15020284.

[18] Imam F, Mukhopadhyay S, Kothiyal P, Alshehri S, Saad Alharbi K, Afzal M, et al. Formulation and characterization of polymeric nanoparticle of Rivastigmine for effective management of Alzheimer's disease. Saudi Pharm J 2024;32:102048. https://doi.org/10.1016/j.jsps.2024.102048.

[19] Ahmad MZ, Sabri AHB, Anjani QK, Domínguez-Robles J, Abdul Latip N, Hamid KA. Design and Development of Levodopa Loaded Polymeric Nanoparticles for Intranasal Delivery. Pharmaceuticals 2022;15:370. https://doi.org/10.3390/ph15030370.

[20] Sun R, Chen Y, Pei Y, Wang W, Zhu Z, Zheng Z, et al. The drug release of PLGA-based nanoparticles and their application in treatment of gastrointestinal cancers. Heliyon 2024;10. https://doi.org/10.1016/j.heliyon.2024.e38165.

[21] Sharma S, Gauba P, Tyagi A, Dang S. Chitosan-modified polymeric nanoparticles for the nose-to-brain drug delivery of paroxetine: an in vitro and in vivo evaluation. Nanoscale 2025;17:1687–702. https://doi.org/10.1039/D4NR04250F.

[22] Rahimpour E, Moradi M, Sheikhi-Sovari A, Rezaei H, Rezaei H, Jouyban-Gharamaleki V, et al. Comparative Drug Solubility Studies Using Shake-Flask Versus a Laser-Based Robotic Method. AAPS PharmSciTech 2023;24:207. https://doi.org/10.1208/s12249-023-02667-9.

[23] Dikpati A, Maio VDP, Ates E, Greffard K, Bertrand N. Studying the stability of polymer nanoparticles by size exclusion chromatography of radioactive polymers. J Controlled Release 2024;369:394–403. https://doi.org/10.1016/j.jconrel.2024.03.053.

[24] Phatak N, Bhattacharya S, Shah D, Manthalkar L, Sreelaya P, Jain A. Cd44 Targeted Delivery of Hyaluronic Acid-Coated Polymeric Nanoparticles Against Colorectal Cancer. Nanomed 2023;18:1613–34. https://doi.org/10.2217/nnm-2023-0145.

[25] Malekpour MR, Hosseindoost S, Madani F, Kamali M, khosravani M, Adabi M. Combination nanochemotherapy of brain tumor using polymeric nanoparticles loaded with doxorubicin and paclitaxel: An in vitro and in vivo study. Eur

J Pharm Biopharm 2023;193:175–86. https://doi.org/10.1016/j.ejpb.2023.11.002.

[26] Vanza JD, Lalani JR, Patel RB, Patel MR. DOE supported optimization of biodegradable polymeric nanoparticles based dry powder inhaler for targeted delivery of afatinib in non-small cell lung cancer. J Drug Deliv Sci Technol 2023;84:104554. https://doi.org/10.1016/j.jddst.2023.104554.

[27] García-Melero J, López-Mitjavila J-J, García-Celma MJ, Rodriguez-Abreu C, Grijalvo S. Rosmarinic Acid-Loaded Polymeric Nanoparticles Prepared by Low-Energy Nano-Emulsion Templating: Formulation, Biophysical Characterization, and In Vitro Studies. Materials 2022;15:4572. https://doi.org/10.3390/ma15134572.

[28] Sakhi M, Khan A, Khan I, Ahmad Khan S, Irum Khan S, Ali Khattak M, et al. Effect of polymeric stabilizers on the size and stability of PLGA paclitaxel nanoparticles. Saudi Pharm J 2023;31:101697. https://doi.org/10.1016/j.jsps.2023.101697.

[29] Kumari V, Tyagi P, Sangal A. *In-Vitro* kinetic release study of *illicium verum (Chakraphool)* polymeric nanoparticles. Mater Today Proc 2022;60:14–20. https://doi.org/10.1016/j.matpr.2021.11.014.

[30] Alenazi ASM, El-Bagory IM, Yassin AB, Alanazi FK, Alsarra IA, Haq N, et al. Design of polymeric nanoparticles for oral delivery of capreomycin peptide using double emulsion technique: Impact of stress conditions. J Drug Deliv Sci Technol 2022;71:103326. https://doi.org/10.1016/j.jddst.2022.103326.

[31] Nouruzi E, Hosseini SM, Asghari B, Mahjoub R, Zare EN, Shahbazi M-A, et al. Effect of poly (lactic-co-glycolic acid) polymer nanoparticles loaded with vancomycin against Staphylococcus aureus biofilm. BMC Biotechnol 2023;23:39. https://doi.org/10.1186/s12896-023-00811-8.

[32] Dols-Perez A, Fornaguera C, Feiner-Gracia N, Grijalvo S, Solans C, Gomila G. Effect of surface functionalization and loading on the mechanical properties of soft polymeric nanoparticles prepared by nano-emulsion templating. Colloids Surf B Biointerfaces 2023;222:113019. https://doi.org/10.1016/j.colsurfb.2022.113019.

[33] Nunes D, Andrade S, Ramalho MJ, Loureiro JA, Pereira MC. Polymeric Nanoparticles-Loaded Hydrogels for Biomedical Applications: A Systematic Review on In Vivo Findings. Polymers 2022;14:1010. https://doi.org/10.3390/polym14051010.

[34] Ortega A, da Silva AB, da Costa LM, Zatta KC, Onzi GR, da Fonseca FN, et al. Thermosensitive and mucoadhesive hydrogel containing curcumin-loaded lipid-core nanocapsules coated with chitosan for the treatment of oral squamous cell carcinoma. Drug Deliv Transl Res 2023;13:642–57. https://doi.org/10.1007/s13346-022-01227-1.

[35] Fu Z, Huang L, Zhang X, Zheng Z, Wu L, Zheng H. Enhanced photothermal therapy for oral cancer using benzothiadiazole-based nanoparticle-loaded hydrogels. Artif Cells Nanomedicine Biotechnol 2025;53:345–60. https://doi.org/10.1080/21691401.2025.2540648.

[36] Zhang RX, Lu W, Yan X, Deng X, Wan R, Song Z, et al. Rectal nanoparticulate-hydrogel delivering budesonide to reduce enterohepatic drug metabolism and clearance. Drug Deliv Transl Res 2026. https://doi.org/10.1007/s13346-026-02095-9.

[37] Yoon MS, Lee JM, Jo MJ, Kang SJ, Yoo MK, Park SY, et al. Dual-Drug Delivery Systems Using Hydrogel–Nanoparticle Composites: Recent Advances and Key Applications. Gels 2025;11:520. https://doi.org/10.3390/gels11070520.

[38] Kesharwani P, Fatima M, Singh V, Sheikh A, Almalki WH, Gajbhiye V, et al. Itraconazole and Difluorinated-Curcumin Containing Chitosan Nanoparticle Loaded Hydrogel for Amelioration of Onychomycosis. Biomimetics 2022;7:206. https://doi.org/10.3390/biomimetics7040206.

[39] Habibi N, Ferdosi-Shahandashti E, Najafzadehvarzi H, Golchoobian R, Babazadeh SZ, Goudarzi MTH. Design and synthesis of gold nanoparticle-loaded hydrogel for stem cell delivery to promote cardiac cell regeneration after myocardial infarction. J Drug Deliv Sci Technol 2026;116:107902. https://doi.org/10.1016/j.jddst.2025.107902.

[40] Wang C, Yang Y, Liang R, Wu S, Xuan C, Lv W, et al. Preparation and anti-inflammatory effect of mercury sulphide nanoparticle-loaded hydrogels. J Drug Target 2024;32:557–69. https://doi.org/10.1080/1061186X.2024.2332729.

[41] Sachin KS, Koshy JT, Sangeetha D. Development of Ag doped ZnO nanoparticle loaded carboxymethyl cellulose/polyvinyl alcohol hydrogel film for enhanced wound dressing. Inorg Chem Commun 2025;178:114606. https://doi.org/10.1016/j.inoche.2025.114606.

[42] Dahiya P, Zafar A, Ahmad FJ, Khalid M, Ali A. Development of Forskolin and rutin-loaded polymeric nanoparticles for enhancement of topical ocular delivery: Optimization, in-vitro, ex-vivo, and toxicity evaluation. J Drug Deliv Sci Technol 2023;82:104292. https://doi.org/10.1016/j.jddst.2023.104292.

[43] Kumar L, Kukreti G, Rana R, Chaurasia H, Sharma A, Sharma N, et al. Poly(lactic-co-glycolic) Acid (PLGA) Nanoparticles and Transdermal Drug Delivery: An Overview. Curr Pharm Des 2023;29:2940–53. https://doi.org/10.2174/0113816128275385231027054743.

[44] Jyothi D, Priya S, James JP. DEVELOPMENT AND OPTIMIZATION OF POLYMERIC NANOPARTICLES OF GLYCYRRHIZIN: PHYSICOCHEMICAL CHARACTERIZATION AND ANTIOXIDANT ACTIVITY. Int J Appl Pharm 2024:166–71. https://doi.org/10.22159/ijap.2024v16i1.49164.

[45] Mahar R, Chakraborty A, Nainwal N, Bahuguna R, Sajwan M, Jakhmola V. Application of PLGA as a Biodegradable and Biocompatible Polymer for Pulmonary Delivery of Drugs. AAPS PharmSciTech 2023;24:39. https://doi.org/10.1208/s12249-023-02502-1.

[46] Raman S, Khan AA, Mahmood S. Nose to brain delivery of selegiline loaded PLGA/lipid nanoparticles: Synthesis, characterisation and brain pharmacokinetics evaluation. J Drug Deliv Sci Technol 2022;77:103923. https://doi.org/10.1016/j.jddst.2022.103923.

[47] Sharma DK, Pattnaik G, Behera A. Development and in-vitro, in-vivo evaluation of Pioglitazone-loaded polymeric nanoparticles using central composite design surface response methodology. OpenNano 2023;11:100141. https://doi.org/10.1016/j.onano.2023.100141.

[48] Mendez-Pfeiffer P, Juarez J, Hernandez J, Taboada P, Virués C, Alday E, et al. Polymeric nanoparticles for the delivery of Sonoran desert propolis: Synthesis, characterization and antiproliferative activity on cancer cells. Colloids Surf B Biointerfaces 2022;215:112475. https://doi.org/10.1016/j.colsurfb.2022.112475.

[49] Jing C, Chen S, Bhatia SS, Li B, Liang H, Liu C, et al. Bone-targeted polymeric nanoparticles as alendronate carriers for potential osteoporosis treatment. Polym Test 2022;110:107584. https://doi.org/10.1016/j.polymertesting.2022.107584.

[50] Gonsalves A, Sorkhdini P, Bazinet J, Ghumman M, Dhamecha D, Zhou Y, et al. Development and characterization of lung surfactant-coated polymer nanoparticles for pulmonary drug delivery. Biomater Adv 2023;150:213430. https://doi.org/10.1016/j.bioadv.2023.213430.